Title

Microfluidic Single-Cell Analysis Shows That Porcine Induced Pluripotent Stem Cell–Derived Endothelial Cells Improve Myocardial Function by Paracrine Activation

Journal

Circulation Research, 111(7)

ISSN

0009-7330

Authors

Gu, Mingxia
Nguyen, Patricia K
Lee, Andrew S
et al.

Publication Date

2012-09-14

DOI

10.1161/circresaha.112.269001

Peer reviewed

Published in final edited form as:
Circ Res. 2012 September 14; 111(7): 882–893. doi:10.1161/CIRCRESAHA.112.269001.

Microfluidic Single Cell Analysis Show Porcine Induced Pluripotent Stem Cell-Derived Endothelial Cells Improve Myocardial Function by Paracrine Activation

Mingxia Gu[1,2,3,*], **Patricia K. Nguyen**[1,*], **Andrew S. Lee**[1,2], **Dan Xu**[1,2], **Shijun Hu**[1,2], **Jordan R Plews**[1,2], **Leng Han**[1,2], **Bruno C. Huber**[1,2], **Won Hee Lee**[1,2], **Yongquan Gong**[1,2,4], **Patricia E. de Almeida**[1,2], **Jennifer Lyons**[1], **Fumi Ikeno**[1], **Cholawat Pacharinsak**[5], **Andrew J. Connolly**[6], **Sanjiv S. Gambhir**[2], **Robert C. Robbins**[4], **Michael T. Longaker**[7], and **Joseph C. Wu**[1,2,8]

[1]Department of Medicine, Division of Cardiology, Stanford University School of Medicine

[2]Department of Radiology, Molecular Imaging Program

[3]Department of Physiology and Pathophysiology, Key Laboratory of Molecular Cardiovascular Sciences of Education Ministry, Peking University Health Sciences Center, Beijing, China

[4]Department of Cardiothoracic Surgery, Stanford

[5]Department of Comparative Medicine, Stanford

[6]Department of Pathology, Stanford

[7]Department of Plastic Surgery, Stanford

[8]Institute of Stem Cell Biology and Regenerative Medicine, Stanford

Abstract

Rationale—Induced pluripotent stem cells (iPSCs) hold great promise for the development of patient-specific therapies for cardiovascular disease. However, clinical translation will require preclinical optimization and validation of large animal iPSC models.

Objective—To successfully derive endothelial cells from porcine iPSCs and demonstrate their potential utility for the treatment of myocardial ischemia.

Methods and Results—Porcine adipose stromal cells were reprogrammed to generate porcine iPSCs (piPSCs). Immunohistochemistry, quantitative PCR, microarray hybridization, and angiogenic assays confirmed that piPSC-derived endothelial cells (piPSC-ECs) shared similar morphological and functional properties as endothelial cells isolated from the autologous pig aorta. To demonstrate their therapeutic potential, piPSC-ECs were transplanted into mice with myocardial infarction (MI). Compared to control, animals transplanted with piPSC-ECs showed significant functional improvement measured by echocardiography (fractional shortening at week 4: 27.2±1.3% vs. 22.3±1.1%; $P<0.001$) and magnetic resonance imaging (ejection fraction at week 4: 45.8±1.3% vs. 42.3±0.9%; $P<0.05$). Quantitative protein assays and microfluidic single cell PCR profiling showed that piPSC-ECs released pro-angiogenic and anti-apoptotic factors in the ischemic microenvironment, which promoted neovascularization and cardiomyocyte survival, respectively. Release of paracrine factors varied significantly among subpopulations of

Address correspondence to: Dr. Joseph C. Wu, 265 Campus Drive, Rm 1120B, Stanford, CA 94305-5344, joewu@stanford.edu. Dr. Michael Longaker, 257 Campus Drive, Stanford, CA 94305-5148, longaker@stanford.edu.
*These authors contributed equally

DISCLOSURES
None

transplanted cells, suggesting that transplantation of specific cell populations may result in greater functional recovery.

Conclusion—In summary, this is the *first* study to successfully differentiate piPSCs-ECs from piPSCs and demonstrate that transplantation of piPSC-ECs improved cardiac function following MI via paracrine activation. Further development of these *large animal* iPSC models will yield significant insights into their therapeutic potential and accelerate the clinical translation of autologous iPSC-based therapy.

Keywords

Induced pluripotent stem cells; large animal models; paracrine activation; myocardial infarction; molecular imaging; ischemic heart disease; vascular biology

INTRODUCTION

In recent years, induced pluripotent stem cells (iPSCs) have become a popular alternative to embryonic stem cells (ESCs) for regenerative medicine.[1, 2] Not only do iPSCs provide an unlimited source of pluripotent cells that are capable of self-renewal, but they also circumvent the ethical concerns associated with ESC derivation and can be transplanted autologously, limiting potential immunologic rejection.[3, 4] To date, iPSCs have been generated from a growing list of species including mice,[5, 6] rats,[7, 8] monkeys,[9] dogs,[10, 11] humans,[12, 13] and pigs,[14, 15] confirming the universality of transgenes for reprogramming.[12, 13] Perhaps the most significant achievement is the development of porcine iPSCs, which can potentially fill the gap between the transplantation of these cells into mice and the initiation of the first clinical trials using iPSCs in humans.

Swine are an ideal large animal model for the clinical translation of experimental medical therapies due to their resemblance to human organ size and physiology and their relatively long lifespan.[16] Consequently, several recent studies have utilized the porcine model as a pre-clinical tool for the clinical translation of cell-based therapy. These studies, however, have been limited to porcine mesenchymal stem cells.[17–20]

It has long been appreciated that endothelial cells play an important role in the survival and function of nearby cardiomyocytes by promoting vascular regeneration and angiogenesis.[21] In the normal heart, capillary networks can be found near almost every cardiomyocyte, modulating cardiac performance, contraction, and growth. Thus, it is not surprising that in the ischemic myocardium, a deficit of blood flow leads to progressive cardiomyocyte death and myocardial dysfunction.[22] To exploit the potential therapeutic benefits of endothelial cells, several investigators have differentiated endothelial cells from iPSCs generated from mice,[23] canine,[11] and humans,[24] demonstrating that paracrine release of pro-angiogenic factors promote functional recovery in small animal models of ischemia. Prior studies, however, have analyzed entire cell populations. Because cell populations are heterogeneous, especially those generated from exogenous factors like iPSCs and their derivatives, it is critical to study the regulation of angiogenesis at the single cell level.

In this study, we lay the foundation for the clinical application of iPSCs for the treatment of ischemic heart disease. After generation of iPSCs from adipose tissue of adult miniswine, we successfully differentiated these cells into endothelial cells that share similar morphological and functional properties to their endogenous counterparts (i.e., endothelial cells isolated from the porcine aorta). We then demonstrated that porcine iPSC-derived endothelial cells (piPSC-ECs) could provide therapeutic benefit in a murine model of myocardial infarction (MI). To explore the biological mechanisms for functional recovery, we showed that piPSC-ECs released both pro-angiogenic and anti-apoptotic factors that

promote neoangiogenesis and cardiomyocyte survival, respectively, at the single cell level using microfluidic dynamic arrays.[25] We then demonstrated that the release of paracrine factors varied among specific subpopulations of iPSC-ECs, suggesting that transplantation of specific cell subpopulations may result in greater functional recovery. Finally, cell delivery and engraftment are monitored using positron emission tomography/computed tomography (PET/CT) as well as magnetic resonance imaging (MRI) in a porcine model of MI, laying the groundwork for the development of future imaging protocols to monitor cell delivery and engraftment in humans.

MATERIALS AND METHODS

Derivation of porcine induced pluripotent stem cells

Porcine adipose tissue was harvested and cultured, as described in detail in the Online Supplemental Methods section. Approximately 1×10^4 porcine adipose stromal cells (pASCs) were seeded onto a 24-well tissue culture dish and maintained with human ASC growth medium. Cells were then transduced with 5 μg/mL polybrene (Sigma) plus individual lentivirus containing Oct4, Sox2, Klf4, and c-MYC in a 4:2:2:1 ratio.[13] On day 6, cells were dissociated with 0.05% trypsin-EDTA (Gibco) and counted with a hemocytometer. Reprogramming of piPSCs was performed on mouse embryonic fibroblast (MEF) feeder cells. Ten thousand cells were then transferred onto a MEF feeder layer in a gelatin-coated 6 well plate and cultured with human ESC growth medium containing knockout DMEM (Invitrogen), 20% knock out FBS (Invitrogen), 2 mM L-Glutamine (Invitrogen), 1× nonessential amino acids (Invitrogen), 1× 2-mercaptoethanol (Invitrogen), 100 units/ml penicillin, 100 μg/ml streptomycin, and 10 ng/ml human beta fibroblast growth factor (bFGF) (Invitrogen). ESC-like colonies with distinct edges appeared on day 13–15. On day 15, positive colonies with ESC-like morphologies were isolated with a glass needle and seeded onto new MEFs. These pASC-derived iPSCs were maintained on MEF feeder layers with iPSC medium containing knockout DMEM (Invitrogen), 20% ES-qualified FBS (Invitrogen), 2 mM L-Glutamine (Invitrogen), 1× nonessential amino acids (Invitrogen), 1× 2-mercaptoethanol (Invitrogen), 100 units/ml penicillin, 100 μg/ml streptomycin, and 50 ng/ml human bFGF (Invitrogen). Each selected colony was then established as one individual pASC-iPSC line. A total of 10 lines from the 5 miniswine were generated.

Differentiation of piPSC-derived endothelial cells

For endothelial cell differentiation, well maintained piPSCs at passage number 25 were treated with type IV collagenase (Invitrogen, Carlsbad, CA) for 15 min at 37°C and transferred to ultra-low attachment plates (Corning Life Sciences, Kennebunk, ME) containing differentiation medium for 2 days.[26] The differentiation medium consisted of DMEM (Invitrogen) containing 20% knockout serum (Invitrogen), 4.5 g/L L-glutamine (Invitrogen), 1% nonessential amino acids (Invitrogen), 0.1 mM 2-mercaptoethanol (Invitrogen), 50 units/ml penicillin (Invitrogen), 50 μg/ml streptomycin (Invitrogen), 10 ng/ml Activin A (R& D systems), and 20 ng/ml bone morphogenetic protein-4 (BMP-4) as described previously.[26] The differentiation medium was supplemented with 25 ng/mL vascular endothelial growth factor (VEGF) (R&D system), 8 ng/mL bFGF (R&D system), and 10 μM TGF-β inhibitor SB431542 (Sigma). The 2-day embryoid bodies (EBs) were then seeded onto 0.5% gelatin-coated dishes and cultured for another 8 days in differentiation media in absence of BMP-4. On day 10, plated EBs were digested and sorted by fluorescence activated cell sorting (FACS) for CD31 positive cells. The CD31 positive cells were collected and seeded into one well of a six-well plate with EGM-2 medium (Lonza).

Quantitative polymerase chain reaction (q-PCR) analysis to confirm pluripotent state in piPSCs

Quantitative PCR was performed after isolation of total RNA and cDNA. Using Taqman Gene Expression Assays, PCR reactions were performed with a StepOnePlus Realtime-PCR 7900 HT System (Applied Biosystems, Foster City, CA). Primers for genes defining pluripotency and confirming germ layer differentiation are listed in Online Table I.

Microarray hybridization and data analysis of piPSCs and piPSC-ECs

Total RNA samples were hybridized to Affymetrix GeneChip Porcine Genome Array, and then normalized and annotated by the Affymetrix® Expression Console™ software. For comparison to our generated lines, we obtained piPSC lines (piPSC-ID4, piPSC-ID6, and piPSC-IC1) from R. Michael Roberts and Toshihiko Ezashi (University of Missouri, Columbia, MO) and are grateful for their contribution. We also obtained the expression data for piPSC lines and fibroblast from Gene Expression Omnibus (GEO, http://www.ncbi.nlm.nih.gov/geo, GSE15472).[27] The Pearson correlation coefficient was calculated for each pair of samples using the expression level of transcripts. For hierarchical clustering, a Pearson correlation for average linkage clustering was used.

Generation of a murine model of myocardial infarction and intramyocardial delivery of therapeutic cells

Ligation of the mid left anterior descending (LAD) artery was performed in 8–10 weeks female NOD SCID mice (Jackson Laboratory) under anesthesia (2–3% inhaled isoflurane) by a single experienced micro surgeon (YG). Survival rate for each surgery group was ~90%. Myocardial blanching and EKG changes confirmed myocardial infarction post ligation. Animals were randomized into 4 groups: (1) phosphate buffered saline (PBS) as control, (2) 1×10^6 pASCs, (3) 1×10^6 pAorta-ECs, and (4) 1×10^6 piPSC-ECs (n=20/group). Immediately after LAD ligation, animals were injected intramyocardially near the peri-infarct zone at 2 different sites using a 31-gauge Hamilton syringe (25 μl per injection). Study protocols were approved by the Stanford Animal Research Committee. Animal care was provided in accordance with the Stanford University School of Medicine guidelines and policies for the use of laboratory animals.

Optical bioluminescence imaging (BLI) and micro positron emission tomography (microPET) for tracking cell fate

Please see Online Supplemental Methods.

Angiogenesis and anti-apoptosis cytokine array following hypoxia exposure

Please see Online Supplemental Methods.

Single cell gene expression profiling of transplanted piPSC-ECs and ASCs

Please see Online Supplemental Methods.

Assessment of paracrine activation by specific subpopulations

Because cell populations of pASC and piPSC-ECs are heterogeneous, we hypothesized that the release of paracrine factors varied by specific cell subpopulations. To investigate this hypothesis, we used single cell expression profiling to analyze the release of paracrine factors by subpopulations of pASCs and piPSC-ECs. One week after transplantation of pASCs and piPSC-ECs into mice undergoing LAD infarction (n=5), we sacrificed the mice and harvested and dissociated their hearts as described above. We then used FACS to isolate subpopulations of cells and sort them into a 96 well 0.2-ml PCR plate based on their

expression of endothelial specific markers, specifically CD31, CD34 and CD144. We then performed single cell gene expression analysis to determine the relative amounts of paracrine factors released by each subpopulation of pASC and piPSC-ECs: 1) $CD31^+/CD34^+/CD144^-$, 2) $CD31^+/CD34^-/CD144^+$, and 3) $CD31^+/CD34^-/CD144^-$. Very few cells expressed all three markers and this sub-population was, therefore, not analyzed.

Tracking transplanted cells in miniswine using positron emission tomography and computed tomography (PET/CT) imaging

Please see Online Supplemental Methods.

Statistical analysis

For analysis of microarray data, a Pearson correlation coefficient was utilized. A P value of <0.05 was considered significant. ANOVA with post hoc testing was used to analyze the differences in qPCR, single cell PCR, angiogenesis and anti-apoptotic cytokine data between groups, percent infarct size by triphenyltetrazolium chloride (TTC), and density of dTd-mediated dUTP nick-end labeling (TUNEL)-positive nuclei. The percent infarct size is calculated by dividing the area of infarct by the total area of the left ventricle. Repeated measures of ANOVA were used to analyze MRI, BLI, and echocardiographic data. All data were expressed as mean±SD.

RESULTS

Derivation of piPSCs from adult miniswine

Porcine adipose stromal cells (pASCs) were harvested and successfully reprogrammed into piPSCs from 5 young adult Yucatan miniswine pigs. Retroviral over-expression of Oct4, Sox2, Klf4, and c-Myc was used in a 4:2:2:1 ratio to induce pluripotency. Compact colonies of cells staining positive for alkaline phosphatase, a universal pluripotent marker (Online Figure IA), were initially observed under bright-field microscopy 15 days after transduction (Figure 1A). Individual colonies were mechanically dissociated using a pulled Pasteur pipette and transferred onto irradiated MEF feeder layers for clonal expansion into distinct cell lines. A total of 10 piPSC lines were generated, 2 lines from each miniswine. piPSC colonies stained positive for Nanog, Oct4, c-Myc, Klf4, and SSEA-1 (Figure 1B) as well as Tra-1-60 and Tra-1-81 (Online Figure IB). By contrast, adult somatic pASCs from which piPSCs were derived revealed very low or no expression of these genes (Figure 1B and Online Figure IB). piPSCs were also characterized by semi-quantitative reverse transcription PCR, which showed up-regulation of pluripotency genes (Figure 1C). Microarray analyses were conducted to determine the degree of similarity between different piPSC lines. Hierarchical clustering of the whole genome expression showed that the generated piPSC lines were highly similar to the piPSC lines derived by Ezashi et al.[27] (piPSC-ID4, piPSC-ID6, and piPSC-IC1), and were distinct from their somatic precursors (pASC) and porcine fibroblasts (pfibroblast-1 and -2) (Figure 1D). Genomic stability of generated piPSCs was demonstrated through karyotyping after extended culture for 40 passages (Online Figure IC).

Confirmation of pluripotency by in vitro and in vivo differentiation

To further confirm the pluripotency of piPSCs derived from pASCs, we differentiated piPSCs *in vitro* by 3-dimensional EB formation. After one week of spontaneous differentiation using the hanging drop assay, piPSCs gave rise to cell types from the three different germ layers, as evidenced by immunostaining and quantitative PCR (Online Figure IIA and B). We then applied the *in vivo* teratoma formation assay as a definitive test to assess pluripotency. We transplanted piPSCs at passage 50 into the kidney capsule of SCID

mice. Palpable tumors were seen 4 weeks after transplantation. Tumors were explanted 10 weeks after injection. Histological examination of the teratoma revealed the presence of derivatives of all three germ layers, including neural epithelium (ectoderm), chondrogenic stroma (mesoderm), and glandular epithelium (endoderm) (Online Figure IIC).

In vivo tracking of teratoma growth by BLI

Teratoma development was tracked *in vivo* to provide further evidence of pluripotency. To track teratoma growth *in vivo*, we stably transduced piPSCs with a lentiviral triple fusion (TF) reporter gene construct containing firefly luciferase (FLuc), monomeric red fluorescent protein (mRFP), and herpes simplex virus truncated thymidine kinase (HSVttk) driven by ubiquitin promoter. Cells expressing the reporter gene were selected by cell sorting for mRFP (Online Figure IIIA). Following injection into the sub-renal capsule of immunodeficient mice, teratoma growth was confirmed by BLI (Online IIIB).

Generation of functional porcine induced pluripotent stem cell-derived endothelial cells

We next tested whether we could differentiate piPSCs into a therapeutic cell population. Transplantation of endothelial cells is known to restore function to ischemic tissues through revascularization.[11, 28, 29] Generation of piPSC-ECs was conducted via directed cell differentiation of EBs followed by FACS for the endothelial cell marker CD31 at day 12 after induction of differentiation (Figure 2A). Cells isolated by sorting stained positive for CD31, exhibited fluorescent Dil (3,3′-dioctadecylindocarbocyanine iodide)-LDL uptake, and formed tubules *in vitro* when plated on Matrigel and *in vivo* using a Matrigel plug assay (Figure 2B and Online Figure IV). Microarray data on gene expression profiles also demonstrated that piPSC-ECs were similar to ECs harvested from the autologous pig aorta endothelial cells (pAorta-ECs) (Figure 2C). Taken together, these data suggest that piPSC-ECs have similar morphological and functional properties to endogenous ECs and, thus, can be used as an alternative therapeutic option for vascular regeneration.

Delivery of piPSC-ECs results in improvement of cardiac function following myocardial infarction

To test the therapeutic efficacy of the piPSC-ECs *in vivo*, we injected 1×10^6 piPSC-ECs into a murine MI model and compared the functional recovery among mice treated with PBS (negative control), 1×10^6 pASCs given their reported therapeutic benefit,[30, 31] and 1×10^6 pAorta-ECs (positive control). Functional recovery was assessed by echocardiography (Figure 3A, B) and MRI (Online Figure V). Significant functional improvement was observed in mice treated with piPSC-ECs compared to PBS control as shown by echocardiography (fractional shortening at week 2, 23.7±0.9% vs. 19.3±0.5%, *P<0.01; week 4, 27.2±1.3% vs. 22.3±1.1%; **P<0.001) and MRI (ejection fraction at week 2, 43.7±1.0% vs. 40.6±0.9%; week 4, 45.8±1.3% vs. 42.3±0.9%; *P<0.05). The PBS group showed a slight increase in EF over time due to recovery from initial myocardial stunning, which has been reported in prior studies using rodent [32, 33] and porcine models of myocardial infarction.[34, 35] Our results consistently showed that piPSC-ECs produced statistically significant functional improvement at week 2 and 4. Short-term engraftment into the myocardium was also confirmed by BLI (Figure 3C) and microPET imaging (Online Figure IIID), which showed focal [^{18}F]FHBG radiotracer uptake in the anterior left ventricle. Interestingly, there was a trend toward greater improvement in fractional shortening in mice injected with piPSC-ECs and pAorta-ECs compared to mice injected with pASCs.

Histological evaluation of transplanted piPSC-ECs into the peri-infarct area

To confirm *in vivo* imaging data, a subset of animals were sacrificed and their hearts were explanted at week 4. On gross histochemical analysis by triphenyltetrazolium chloride (TTC) (Figure 4A and B), animals treated with piPSC-ECs showed smaller average infarct area when compared to control (25.2±1.5% vs. 32.7±0.8%; $P<0.05$). Similarly, microscopic analysis by hematoxylin and eosin (H&E) staining showed thicker left ventricular walls in mice treated with piPSC-ECs compared to the control group (281±12 μm vs. 161±6 μm; $P<0.05$) (Figure 4C and D). Immunohistochemistry of the peri-infarct area by mouse CD31 staining showed the number of capillaries per high power field was higher in the group receiving piPSC-ECs than those receiving PBS (395±28 vessels/mm^2 vs. 107±9 vessels/mm^2; $P<0.05$) (Figure 4E and F), suggesting that neovascularization may be a potential mechanism for improvement in cardiac function and decreased scar size. To evaluate whether the piPSC-ECs can form mature and functional vessels in the mouse infarction model and contribute to neovascularization, we performed immunofluorescence staining with anti-porcine CD31 antibodies (green) and anti-murine CD31 antibodies (red) in areas of increased capillary formation from explanted murine hearts. We found that microvessels were only immunoreactive to murine-specific antibodies (Online Figure VIA and B). However, piPSC-ECs could be found surrounding murine microvessels even though the cells themselves do not form mature vessels in hearts explanted 4 weeks after transplantation (Online Figure VIC and D). The coalescing of piPSC-ECs adjacent to murine microvessels supports our findings that piPSC-ECs release pro-angiogenic factors that increase native vessel formation. The failure of piPSC-ECs to form discrete microvessels in the mouse infarcted heart may be due to an insufficient number of piPSC-ECs present in the infarcted mouse heart to support vessel formation. As shown by bioluminescence imaging (Figure 3C), the majority of transplanted piPSC-ECs do not survive 4 weeks post-transplantation. In contrast, formation of discrete microvessels was demonstrated by the *in vivo* Matrigel plug assay seven days after implantation, which is a very different environmental niche (Online Figure IV),

Assessment of paracrine factor release in vitro by piPSC-ECs in response to hypoxia

Given that the majority of cells do not survive 4 weeks post transplantation (Figure 3C), we hypothesize that piPSC-ECs may release paracrine factors that promote angiogenesis in the setting of ischemia, accounting for the longer-term functional benefit that was observed. To explore this hypothesis, we compared the secretion of pro-angiogenic cytokines in pASC, pAorta-ECs, and piPSC-ECs after 24 hours of hypoxia (Figure 5). The culture medium served as control. Both pASCs and piPSC-ECs secreted more angiogenic factors than control. In addition, piPSC-ECs secreted more TNF-α, FGF-β, IL-1α, IL-6, IL-8, and Leptin than pASCs (*$P<0.05$, **$P<0.01$ vs. pASCs). The pattern of cytokine secretion was similar between piPSC-ECs and pAorta-ECs. Taken together, these *in vitro* data suggest that piPSC-ECs can provide a framework for new vessel growth via secretion of paracrine factors regulating angiogenesis.

Single cell profiling of transplanted piPSC-ECs reveals in vivo paracrine activation

Because of the heterogeneous nature of all cell populations, especially those derived from exogenous factors such as piPSCs and their derivatives,[36] it is important to study the expression of pro-angiogenic genes at the single cell level. In addition, it is also necessary to confirm that piPSC-ECs release paracrine factors under ischemic conditions *in vivo.* To meet these objectives, we injected the piPSC-ECs into the peri-infarct zone of murine hearts after MI or into the same anatomical location of control mice with non-infarct sham surgery. After enzymatic digestion of explanted hearts into single cell suspension, we performed FACS for mRFP expression by piPSC-ECs. Individually isolated piPSC-ECs transplanted into ischemic vs. non-ischemic hearts were analyzed by expression of 13 common

angiogenic genes using the microfluidic single cell PCR platform (Figure 6A and B). A number of genes were highly expressed in the piPSC-ECs injected into the peri-infarct zone compared with cells injected into the non-injured myocardium, including VEGFA, IL-6, IL-10, TNF, IFNA1, TIMP1, TIMP2, GATA4, ANGPT1, and CSF3 (ischemia vs. sham; *P<0.05, **P<0.001). These results correlated well with our *in vitro* findings that piPSC-ECs were capable of secreting a series of angiogenic factors under hypoxic conditions, accounting for the functional improvement observed in animals treated with piPSC-ECs. Because populations of pASCs and piPSC-ECs are heterogeneous, we characterized the pattern of paracrine secretion by different cell subpopulations (CD31+/CD34+/CD144− vs. CD31+/CD34-/CD144+ vs. CD31+/CD34-/CD144-) using single cell qRT-PCR analysis. We found that the release of paracrine factors varied among different subpopulations of pASC and piPSC-ECs (Figure 6C and D). We also found that cells expressing CD34 and CD144 released more pro-angiogenic and anti-apoptotic factors than other subpopulations of piPSC-ECs and pASCs. These data suggest that greater functional recovery may be achieved by transplanting a select population of cells rather than a heterogeneous mixture of cells.

Transplanted piPSC-ECs inhibit apoptosis by TUNEL staining

Interestingly, the same angiogenic genes (i.e., VEGF-A, IL6, IL10, TIMP1, GATA4, ANGPT1, and CSF3) that are up-regulated in the peri-infarct zone post piPSC-EC transplantation also play an important role in regulating apoptosis and promoting cell survival. To explore whether the transplantation of piPSC-ECs inhibited cardiomyocyte and endothelial cell apoptosis, we measured the amount of DNA fragmentation in explanted hearts of treated and control animals (n=3 animals per group) using the TUNEL assay. The density of TUNEL-positive nuclei, shown as the percentage of total nuclei, was significantly lower in mice transplanted with piPSC-ECs compared to PBS control (6.1±0.6% vs. 18.9±0.9%, P=0.002). These findings suggest that inhibition of apoptosis by piPSC-ECs may also contribute to functional recovery (Online Figure VII).

Imaging piPSC fate in a porcine model of myocardial infarction using PET/CT and MRI

Prior to clinical application of iPSCs in humans, successful delivery and monitoring of cells in a large animal model must first be established. Swine are an ideal large animal model for the clinical translation of iPSC-based therapy due to their resemblance to human organ size and physiology and their relatively long lifespan.[16] To demonstrate feasibility of tracking piPSCs in swine using PET/CT and MRI, we injected piPSCs into Yucatan miniswine that previously underwent LAD balloon catheter occlusion to induce a myocardial infarction (Online Video I). Prior to intramyocardial cell transplantation, piPSCs were directly labeled with [^{18}F]-FDG for PET imaging, iron particles for co-localization with MRI, and a fluorescent carbocyanine dye for histological identification. We chose direct labeling of cells with [^{18}F]-FDG rather than reporter gene imaging due to the robustness of this technique and its application in current clinical trials.[37–39] Following intramyocardial delivery of 2×10^8 piPSCs into the peri-infarct area under direct visualization, PET/CT and MRI demonstrated that transplanted cells localized to the peri-infarct area of the apical lateral wall of the left ventricle (Online Figure VIIIA and B). After imaging, hearts were explanted and immunofluorescence staining demonstrated the presence of cells expressing the carbocyanine dye (*red*) as well as the pluripotent marker Oct-4 (*green*) in the peri-infarct area (Online Figure VIIIC). Histology revealed piPSCs with a large nucleus and abundant cytoplasm in the peri-infarct area (Online Figure VIIID).

DISCUSSION

Because swine have a close resemblance to humans in terms of anatomy and physiology, the results of this study have several important implications for the clinical translation of iPSC

therapy. First, we have shown that piPSCs can be successfully differentiated into a therapeutic cell population that mimics their endogenous counterparts, paving the way for the development of additional therapeutic subtypes. Second, we have demonstrated that the therapeutic effectiveness of piPSC-ECs in repairing the damaged myocardium is mediated by the release of pro-angiogenic and anti-apoptotic modulating factors, using a novel microfluidic single cell analysis. Third, we have also shown that the release of paracrine factors is highest among the subpopulation of piPSC-ECS expressing the endothelial specific markers CD34 and CD144, suggesting that transplantation of a subpopulation of these cells may lead to greater functional recovery. Finally, we have provided further validation of *in vivo* noninvasive multimodality imaging, facilitating the future development of imaging protocols to guide the delivery and monitoring of iPSC derivatives.

Large animal iPSCs have been recently derived from a number of species including monkeys,[9] dogs,[10, 11] humans,[12, 13] and pigs[14, 15]. Successful differentiation of these cells into therapeutic cell populations, however, is necessary to harness the clinical potential of iPSC technology. Surprisingly, except for human iPSCs, reports on large animal iPSC differentiation into therapeutic cell types for the treatment of cardiovascular disease have been limited. Using a modified protocol designed for human iPSC-EC differentiation,[26] we generated piPSC-ECs that were morphologically and functionally similar to endothelial cells harvested from the autologous porcine aorta, based on standard *in vitro* and *in vivo* assays. Interestingly, these cells secrete paracrine factors at comparable levels and improve cardiac function to a similar extent as their endogenous counterparts. Although cell transplantation with native endothelial cells has been shown to promote angiogenesis and improve cardiac function,[40] we believe that iPSC derivatives are a superior alternative because they have a potentially unlimited source unlike native endogenous endothelial cells, which are challenging to harvest and have a restricted supply. However, further optimization and modification of established human differentiation protocols are still needed for efficiently generating large quantities of piPSC derivatives such as endothelial cells or cardiomyocytes.[41, 42]

Although the debate continues over the optimal stem cell type for the clinical application of cardiac regenerative therapy, iPSCs appear promising because of their unlimited supply, immune privilege via autologous transplantation, and lack of ethical or regulatory hurdles impeding their clinical application.[43] These cells may also be more effective than other cell types, such as adult somatic stem cells, which have been most often applied in preclinical and clinical trials to date. The efficacy of ASCs, for example, has been demonstrated in several studies with reported benefits due to the secretion of paracrine factors promoting angiogenesis and cell survival.[30] Our head-to-head comparison revealed that piPSC-ECs secrete significantly more pro-angiogenic and anti-apoptotic modulating cytokines than pASCs *in vitro*, a finding that is analogous to a recent report showing that iPSC-derived mesenchymal cells release more paracrine factors than adult bone marrow stem cells.[44] Findings from our *in vivo* study confirmed that transplantation of piPSC-ECs resulted in more neovascularization in the peri-infarct area than transplantation of pASCs. Additional studies directly comparing the efficacy of different stem cell types, however, are needed to determine the best option for clinical translation.

The release of cytokines and growth factors that promote neovascularization and cytoprotection has emerged as a leading mechanism to explain the observed functional improvement post stem cell therapy,[45] in light of results from numerous studies demonstrating poor long-term survival and engraftment of transplanted cells and a paucity of newly generated cardiomyocytes.[46] Improvement in cardiac function has been associated with stem cell induced release of VEGF, IL1-α, IL6, TNF-α, FGF-β, TIMP1, TIMP2, and ANGTP1,[45] all of which were significantly increased in our study. Importantly, in a porcine

model of myocardial infarction, Doyle et al. found that pigs treated with conditioned media containing paracrine factors produced equivalent improvement in regional myocardial function and mass compared to those treated with transplanted cells; recovery was attenuated after administration of cytokine specific antibodies.[34] Interestingly, Cho et al. found that transplanted cells not only directly release cytokines, but also induced the release of these factors from host tissues that is sustained for greater than two weeks, much longer than donor derived factors.[47]

Previous findings, however, have been performed in whole cell populations, which are heterogeneous, and may reflect the average gene expression profile, not necessarily the expression profile of the cells of interest. Because whole cell populations of iPSCs and their derivatives are even more heterogeneous than other stem cell types,[36] perhaps as a result of limitations in reprogramming, variations in differentiation, and/or persistent donor cell memory,[48, 49] we used a novel microfluidic platform to examine gene expression at a single cell level. We confirmed that transplanted piPSC-ECs release pro-angiogenic and anti-apoptotic modulators that lead to new vessel formation, decreased apoptosis, and significant functional recovery of injured myocardium.[50] Despite these encouraging results, further research is needed to define methods to improve survival and engraftment of transplanted cells, which will not only enhance paracrine release of these beneficial factors, but also promote cardiac regeneration.

Because of the heterogeneous nature of iPSC derivatives, we also compared the pattern of paracine release from different subpopulations, specifically cells expressing the endothelial specific markers CD34 and CD144 (or VE-cadherin). Single cell expression analysis revealed that piPSC-ECs expressing either CD34 or CD144 released more pro-angiogenic and anti-apoptotic factors than other subpopulations of piPSC-ECs and pASCs. This is not surprising given the function of these proteins in vasculogenesis. CD34 is a transmembrane protein that is expressed on early hematopoietic precursors and vascular associated structures.[51] CD144 (VE-cadherin) is an endothelial specific adhesion molecule that maintains and controls endothelial cell-to-cell adhesion, and, thus, can regulate vascular permeability and leukocyte extravasation.[52] In addition, it regulates cell proliferation, apoptosis, and the function of vascular endothelial growth factor, making it is essential for embryonic angiogenesis. Furthermore, previous studies have shown that endothelial progenitor cells expressing CD34 and CD144 augment angiogenesis by release of paracrine factors.[53] Given our findings that cells expressing these markers release more pro-angiogenic and anti-apoptotic factors than other subpopulations, future studies should consider transplantation of specific iPSC-derivative cell subpopulations to further enhance functional recovery.

Finally, the development of a robust platform for noninvasive *in vivo* imaging in large animals is critical to ensure that therapeutic cells have been safely delivered near the target area of injury and have integrated into the target tissue.[39] Here we directly labeled cells with [^{18}F]-FDG and iron particles for *in vivo* monitoring by PET/CT and MRI, respectively. Previous studies have reported successful monitoring of cell engraftment in large animals using these approaches, albeit with other stem cell subtypes.[37–39] Similarly, we demonstrate the feasibility of this approach for monitoring the piPSC delivery and engraftment into the peri-infarct area. A major limitation of our study is that we did not evaluate the functional efficacy of piPSC-ECs in a porcine model. This is primarily due to the large number of animals that would be needed to demonstrate robust statistical differences, which would need to be carefully evaluated in follow-up studies. Future studies could also determine whether a dual approach using direct labeling and reporter gene expression could exploit the advantages of both techniques to monitor stem cell delivery in large animals.

In summary, we successfully derived piPSCs and differentiated them into piPSC-ECs, which share similar morphological and functional properties to their endogenous counterparts. We found that piPSC-EC therapy promotes pro-angiogenic and anti-apoptotic cytokine release *in vitro and in vivo*, leading to improved cardiac function in ischemic injury models. We also used multimodality noninvasive imaging to monitor cell engraftment into the peri-infarct area in small and large animal models of myocardial infarction. Taken together, our study provides preclinical validation and optimization of piPSCs-ECs as an effective therapeutic cell population, laying the groundwork for the eventual application of autologous iPSC-based therapy in the future.

Supplementary Material

Refer to Web version on PubMed Central for supplementary material.

Acknowledgments

We would like to thank C. Dana Bangs for performing the cytogenetic analysis for this study. We are grateful to the Stanford Functional Genomics Facility for their assistance with the microarray experiment.

SOURCES OF FUNDING

We thank the NIH DP2 OD004437, NIH RC1 HL099117, NIH R01 EB009689, NIH R33 HL0890267 (JCW), NIH RC1 HL100490 (MTL), U01 HL099776 (RCR), and the American College of Cardiology Foundation GE Healthcare Career Development Award (PKN) for funding support for this study.

Non-standard Abbreviations

ANGT1	angiopoietin 1
ANGT2	angiopoietin 2
BCL2	B-cell lymphoma 2
BLI	bioluminescence imaging
CSF3	colony stimulating factor 3
CT	computed tomography
EBs	embryoid bodies
ECs	endothelial cells
EF	ejection fraction
FACS	fluorescence activated cell sorting
FGF-β	fibroblast growth factor beta
FGFR2	fibroblast growth receptor 2
FLuc	firefly luciferase
H&E	hematoxylin and eosin
HSVttk	herpes simplex virus truncated thymidine kinase
IFNA1	interferon alpha 1
IFN-γ	interferon gamma
IL-1α	interleukin 1 alpha
IL6	interleukin 6

IL8	interleukin 8
IL-10	interleukin 10
IL12	interleukin 12
Ip10	interferon-inducible protein
iPSCs	induced pluripotent stem cells
LAD	left anterior descending artery
MEF	mouse embryonic fibroblast
MI	myocardial infarction
mRFP	monomeric red fluorescent protein
MRI	magnetic resonance imaging
NS	non significant
pAorta-ECs	endothelial cells harvested from the porcine aorta
pASC	porcine adipose stromal cells
PBS	phosphate buffered saline
PCR	polymerase chain reaction
PET	positron emission tomography
Pfibroblasts	porcine fibroblasts
piPSC-ECs	endothelial cells derived from porcine induced pluripotent stem cells
PIGF	placental growth factor
qtRT-PCR	quantitative reverse transcription polymerase chain reaction
TIMP1	tissue inhibitor of metalloproteinase 1
TIMP2	tissue inhibitor of metalloproteinase 2
TF	triple fusion
TNF-α	tumor necrosis factor alpha
TTC	triphenyltetrazolium chloride
VEGF	vascular endothelial growth factor

References

1. Narsinh K, Narsinh KH, Wu JC. Derivation of human induced pluripotent stem cells for cardiovascular disease modeling. Circ Res. 2011; 108:1146–1156. [PubMed: 21527744]
2. Yamanaka S. Induced pluripotent stem cells: past, present, and future. Cell Stem Cell. 2012; 10:678–684. [PubMed: 22704507]
3. Pearl JI, Lee AS, Leveson-Gower DB, Sun N, Ghosh Z, Lan F, Ransohoff J, Negrin RS, Davis MM, Wu JC. Short-term immunosuppression promotes engraftment of embryonic and induced pluripotent stem cells. Cell Stem Cell. 2011; 8:309–317. [PubMed: 21362570]
4. Zhao T, Zhang ZN, Rong Z, Xu Y. Immunogenicity of induced pluripotent stem cells. Nature. 2011; 474:212–215. [PubMed: 21572395]
5. Aoi T, Yae K, Nakagawa M, Ichisaka T, Okita K, Takahashi K, Chiba T, Yamanaka S. Generation of pluripotent stem cells from adult mouse liver and stomach cells. Science. 2008; 321:699–702. [PubMed: 18276851]

6. Okita K, Nakagawa M, Hyenjong H, Ichisaka T, Yamanaka S. Generation of mouse induced pluripotent stem cells without viral vectors. Science. 2008; 322:949–953. [PubMed: 18845712]
7. Hamanaka S, Yamaguchi T, Kobayashi T, Kato-Itoh M, Yamazaki S, Sato H, Umino A, Wakiyama Y, Arai M, Sanbo M, Hirabayashi M, Nakauchi H. Generation of germline-competent rat induced pluripotent stem cells. PLoS One. 2011; 6:e22008. [PubMed: 21789202]
8. Liao J, Cui C, Chen S, Ren J, Chen J, Gao Y, Li H, Jia N, Cheng L, Xiao H, Xiao L. Generation of induced pluripotent stem cell lines from adult rat cells. Cell Stem Cell. 2009; 4:11–15. [PubMed: 19097959]
9. Liu H, Zhu F, Yong J, Zhang P, Hou P, Li H, Jiang W, Cai J, Liu M, Cui K, Qu X, Xiang T, Lu D, Chi X, Gao G, Ji W, Ding M, Deng H. Generation of induced pluripotent stem cells from adult rhesus monkey fibroblasts. Cell Stem Cell. 2008; 3:587–590. [PubMed: 19041774]
10. Luo J, Suhr ST, Chang EA, Wang K, Ross PJ, Nelson LL, Venta PJ, Knott JG, Cibelli JB. Generation of leukemia inhibitory factor and basic fibroblast growth factor-dependent induced pluripotent stem cells from canine adult somatic cells. Stem Cells Dev. 2011; 20:1669–1678. [PubMed: 21495906]
11. Lee AS, Xu D, Plews JR, Nguyen PK, Nag D, Lyons JK, Han L, Hu S, Lan F, Liu J, Huang M, Narsinh KH, Long CT, de Almeida PE, Levi B, Kooreman N, Bangs C, Pacharinsak C, Ikeno F, Yeung AC, Gambhir SS, Robbins RC, Longaker MT, Wu JC. Preclinical derivation and imaging of autologously transplanted canine induced pluripotent stem cells. J Biol Chem. 2011; 286:32697–32704. [PubMed: 21719696]
12. Park IH, Zhao R, West JA, Yabuuchi A, Huo H, Ince TA, Lerou PH, Lensch MW, Daley GQ. Reprogramming of human somatic cells to pluripotency with defined factors. Nature. 2008; 451:141–146. [PubMed: 18157115]
13. Sun N, Panetta NJ, Gupta DM, Wilson KD, Lee A, Jia F, Hu S, Cherry AM, Robbins RC, Longaker MT, Wu JC. Feeder-free derivation of induced pluripotent stem cells from adult human adipose stem cells. Proc Natl Acad Sci U S A. 2009; 106:15720–15725. [PubMed: 19805220]
14. Ezashi T, Matsuyama H, Telugu BP, Roberts RM. Generation of colonies of induced trophoblast cells during standard reprogramming of porcine fibroblasts to induced pluripotent stem cells. Biol Reprod. 2011; 85:779–787. [PubMed: 21734265]
15. West FD, Terlouw SL, Kwon DJ, Mumaw JL, Dhara SK, Hasneen K, Dobrinsky JR, Stice SL. Porcine induced pluripotent stem cells produce chimeric offspring. Stem Cells Dev. 2010; 19:1211–1220. [PubMed: 20380514]
16. Prather RS, Shen M, Dai Y. Genetically modified pigs for medicine and agriculture. Biotechnol Genet Eng Rev. 2008; 25:245–265. [PubMed: 21412358]
17. Amado LC, Saliaris AP, Schuleri KH, St John M, Xie JS, Cattaneo S, Durand DJ, Fitton T, Kuang JQ, Stewart G, Lehrke S, Baumgartner WW, Martin BJ, Heldman AW, Hare JM. Cardiac repair with intramyocardial injection of allogeneic mesenchymal stem cells after myocardial infarction. Proc Natl Acad Sci U S A. 2005; 102:11474–11479. [PubMed: 16061805]
18. Gyöngyösi M, Blanco J, Marian T, Tron L, Petnehazy O, Petrasi Z, Hemetsberger R, Rodriguez J, Font G, Pavo IJ, Kertesz I, Balkay L, Pavo N, Posa A, Emri M, Galuska L, Kraitchman DL, Wojta J, Huber K, Glogar D. Serial noninvasive in vivo positron emission tomographic tracking of percutaneously intramyocardially injected autologous porcine mesenchymal stem cells modified for transgene reporter gene expression. Circ Cardiovasc Imaging. 2008; 1:94–103. [PubMed: 19808526]
19. Lim SY, Kim YS, Ahn Y, Jeong MH, Hong MH, Joo SY, Nam KI, Cho JG, Kang PM, Park JC. The effects of mesenchymal stem cells transduced with Akt in a porcine myocardial infarction model. Cardiovasc Res. 2006; 70:530–542. [PubMed: 16563361]
20. Johnston PV, Sasano T, Mills K, Evers R, Lee ST, Smith RR, Lardo AC, Lai S, Steenbergen C, Gerstenblith G, Lange R, Marban E. Engraftment, differentiation, and functional benefits of autologous cardiosphere-derived cells in porcine ischemic cardiomyopathy. Circulation. 2009; 120:1075–1083. 1077 p following 1083. [PubMed: 19738142]
21. Narmoneva DA, Vukmirovic R, Davis ME, Kamm RD, Lee RT. Endothelial cells promote cardiac myocyte survival and spatial reorganization: implications for cardiac regeneration. Circulation. 2004; 110:962–968. [PubMed: 15302801]

22. Brutsaert DL. Cardiac endothelial-myocardial signaling: its role in cardiac growth, contractile performance, and rhythmicity. Physiol Rev. 2003; 83:59–115. [PubMed: 12506127]
23. Joo HJ, Kim H, Park SW, Cho HJ, Kim HS, Lim DS, Chung HM, Kim I, Han YM, Koh GY. Angiopoietin-1 promotes endothelial differentiation from embryonic stem cells and induced pluripotent stem cells. Blood. 2011; 118:2094–2104. [PubMed: 21680798]
24. Li Z, Suzuki Y, Huang M, Cao F, Xie X, Connolly AJ, Yang PC, Wu JC. Comparison of reporter gene and iron particle labeling for tracking fate of human embryonic stem cells and differentiated endothelial cells in living subjects. Stem Cells. 2008; 26:864–873. [PubMed: 18218820]
25. Sanchez-Freire V, Ebert AD, Kalisky T, Quake SR, Wu JC. Microfluidic single-cell real-time PCR for comparative analysis of gene expression patterns. Nat Protoc. 2012; 7:829–838. [PubMed: 22481529]
26. James D, Nam HS, Seandel M, Nolan D, Janovitz T, Tomishima M, Studer L, Lee G, Lyden D, Benezra R, Zaninovic N, Rosenwaks Z, Rabbany SY, Rafii S. Expansion and maintenance of human embryonic stem cell-derived endothelial cells by TGFbeta inhibition is Id1 dependent. Nat Biotechnol. 2010; 28:161–166. [PubMed: 20081865]
27. Ezashi T, Telugu BP, Alexenko AP, Sachdev S, Sinha S, Roberts RM. Derivation of induced pluripotent stem cells from pig somatic cells. Proc Natl Acad Sci U S A. 2009; 106:10993–10998. [PubMed: 19541600]
28. Li Z, Wu JC, Sheikh AY, Kraft D, Cao F, Xie X, Patel M, Gambhir SS, Robbins RC, Cooke JP. Differentiation, survival, and function of embryonic stem cell derived endothelial cells for ischemic heart disease. Circulation. 2007; 116:I46–54. [PubMed: 17846325]
29. Yamahara K, Sone M, Itoh H, Yamashita JK, Yurugi-Kobayashi T, Homma K, Chao TH, Miyashita K, Park K, Oyamada N, Sawada N, Taura D, Fukunaga Y, Tamura N, Nakao K. Augmentation of neovascularization in hindlimb ischemia by combined transplantation of human embryonic stem cells-derived endothelial and mural cells. PLoS One. 2008; 3:e1666. [PubMed: 18301744]
30. Gimble JM, Katz AJ, Bunnell BA. Adipose-derived stem cells for regenerative medicine. Circ Res. 2007; 100:1249–1260. [PubMed: 17495232]
31. Schenke-Layland K, Strem BM, Jordan MC, Deemedio MT, Hedrick MH, Roos KP, Fraser JK, Maclellan WR. Adipose tissue-derived cells improve cardiac function following myocardial infarction. J Surg Res. 2009; 153:217–223. [PubMed: 18694573]
32. Nakamura Y, Wang X, Xu C, Asakura A, Yoshiyama M, From AH, Zhang J. Xenotransplantation of long-term-cultured swine bone marrow-derived mesenchymal stem cells. Stem Cells. 2007; 25:612–620. [PubMed: 17095707]
33. Fernandes S, Naumova AV, Zhu WZ, Laflamme MA, Gold J, Murry CE. Human embryonic stem cell-derived cardiomyocytes engraft but do not alter cardiac remodeling after chronic infarction in rats. J Mol Cell Cardiol. 2010; 49:941–949. [PubMed: 20854826]
34. Doyle B, Sorajja P, Hynes B, Kumar AH, Araoz PA, Stalboerger PG, Miller D, Reed C, Schmeckpeper J, Wang S, Liu C, Terzic A, Kruger D, Riederer S, Caplice NM. Progenitor cell therapy in a porcine acute myocardial infarction model induces cardiac hypertrophy, mediated by paracrine secretion of cardiotrophic factors including TGFbeta1. Stem Cells Dev. 2008; 17:941–951. [PubMed: 18564032]
35. Xiong Q, Hill KL, Li Q, Suntharalingam P, Mansoor A, Wang X, Jameel MN, Zhang P, Swingen C, Kaufman DS, Zhang J. A fibrin patch-based enhanced delivery of human embryonic stem cell-derived vascular cell transplantation in a porcine model of postinfarction left ventricular remodeling. Stem Cells. 2011; 29:367–375. [PubMed: 21732493]
36. Narsinh KH, Sun N, Sanchez-Freire V, Lee AS, Almeida P, Hu S, Jan T, Wilson KD, Leong D, Rosenberg J, Yao M, Robbins RC, Wu JC. Single cell transcriptional profiling reveals heterogeneity of human induced pluripotent stem cells. J Clin Invest. 2011; 121:1217–1221. [PubMed: 21317531]
37. Doyle B, Kemp BJ, Chareonthaitawee P, Reed C, Schmeckpeper J, Sorajja P, Russell S, Araoz P, Riederer SJ, Caplice NM. Dynamic tracking during intracoronary injection of 18F-FDG-labeled progenitor cell therapy for acute myocardial infarction. J Nucl Med. 2007; 48:1708–1714. [PubMed: 17909258]

38. Kang WJ, Kang HJ, Kim HS, Chung JK, Lee MC, Lee DS. Tissue distribution of 18F-FDG-labeled peripheral hematopoietic stem cells after intracoronary administration in patients with myocardial infarction. J Nucl Med. 2006; 47:1295–1301. [PubMed: 16883008]
39. Nguyen PK, Lan F, Wang Y, Wu JC. Imaging: guiding the clinical translation of cardiac stem cell therapy. Circ Res. 2011; 109:962–979. [PubMed: 21960727]
40. Okada M, Payne TR, Zheng B, Oshima H, Momoi N, Tobita K, Keller BB, Phillippi JA, Peault B, Huard J. Myogenic endothelial cells purified from human skeletal muscle improve cardiac function after transplantation into infarcted myocardium. J Am Coll Cardiol. 2008; 52:1869–1880. [PubMed: 19038685]
41. Ren Y, Lee MY, Schliffke S, Paavola J, Amos PJ, Ge X, Ye M, Zhu S, Senyei G, Lum L, Ehrlich BE, Qyang Y. Small molecule Wnt inhibitors enhance the efficiency of BMP-4-directed cardiac differentiation of human pluripotent stem cells. J Mol Cell Cardiol. 2011; 51:280–287. [PubMed: 21569778]
42. Burridge PW, Keller G, Gold JD, Wu JC. Production of de novo cardiomyocytes: human pluripotent stem cell differentiation and direct reprogramming. Cell Stem Cell. 2012; 10:16–28. [PubMed: 22226352]
43. Sun N, Longaker MT, Wu JC. Human iPS cell-based therapy: Considerations before clinical applications. Cell Cycle. 2010; 9:880–885. [PubMed: 20160515]
44. Lian Q, Zhang Y, Zhang J, Zhang HK, Wu X, Lam FF, Kang S, Xia JC, Lai WH, Au KW, Chow YY, Siu CW, Lee CN, Tse HF. Functional mesenchymal stem cells derived from human induced pluripotent stem cells attenuate limb ischemia in mice. Circulation. 2010; 121:1113–1123. [PubMed: 20176987]
45. Gnecchi M, Zhang Z, Ni A, Dzau VJ. Paracrine mechanisms in adult stem cell signaling and therapy. Circ Res. 2008; 103:1204–1219. [PubMed: 19028920]
46. Laflamme MA, Chen KY, Naumova AV, Muskheli V, Fugate JA, Dupras SK, Reinecke H, Xu C, Hassanipour M, Police S, O'Sullivan C, Collins L, Chen Y, Minami E, Gill EA, Ueno S, Yuan C, Gold J, Murry CE. Cardiomyocytes derived from human embryonic stem cells in pro-survival factors enhance function of infarcted rat hearts. Nat Biotechnol. 2007; 25:1015–1024. [PubMed: 17721512]
47. Cho HJ, Lee N, Lee JY, Choi YJ, Ii M, Wecker A, Jeong JO, Curry C, Qin G, Yoon YS. Role of host tissues for sustained humoral effects after endothelial progenitor cell transplantation into the ischemic heart. J Exp Med. 2007; 204:3257–3269. [PubMed: 18070934]
48. Ghosh Z, Wilson KD, Wu Y, Hu S, Quertermous T, Wu JC. Persistent donor cell gene expression among human induced pluripotent stem cells contributes to differences with human embryonic stem cells. PLoS One. 2010; 5:e8975. [PubMed: 20126639]
49. Kim K, Doi A, Wen B, Ng K, Zhao R, Cahan P, Kim J, Aryee MJ, Ji H, Ehrlich LI, Yabuuchi A, Takeuchi A, Cunniff KC, Hongguang H, McKinney-Freeman S, Naveiras O, Yoon TJ, Irizarry RA, Jung N, Seita J, Hanna J, Murakami P, Jaenisch R, Weissleder R, Orkin SH, Weissman IL, Feinberg AP, Daley GQ. Epigenetic memory in induced pluripotent stem cells. Nature. 2010; 467:285–290. [PubMed: 20644535]
50. Quevedo HC, Hatzistergos KE, Oskouei BN, Feigenbaum GS, Rodriguez JE, Valdes D, Pattany PM, Zambrano JP, Hu Q, McNiece I, Heldman AW, Hare JM. Allogeneic mesenchymal stem cells restore cardiac function in chronic ischemic cardiomyopathy via trilineage differentiating capacity. Proc Natl Acad Sci U S A. 2009; 106:14022–14027. [PubMed: 19666564]
51. Furness SG, McNagny K. Beyond mere markers: functions for CD34 family of sialomucins in hematopoiesis. Immunol Res. 2006; 34:13–32. [PubMed: 16720896]
52. Vestweber D. VE-cadherin: the major endothelial adhesion molecule controlling cellular junctions and blood vessel formation. Arterioscler Thromb Vasc Biol. 2008; 28:223–232. [PubMed: 18162609]
53. Sieveking DP, Buckle A, Celermajer DS, Ng MK. Strikingly different angiogenic properties of endothelial progenitor cell subpopulations: insights from a novel human angiogenesis assay. J Am Coll Cardiol. 2008; 51:660–668. [PubMed: 18261686]

Novelty and Significance

What Is Known?

- Induced pluripotent stem cells (iPSCs) have been created from adult somatic cells of many small and large animals.
- More recently, iPSCs have been derived from swine, an animal that shares a similar cardiovascular anatomy and physiology to humans.

What New Information Does This Study Contribute?

- We successfully created iPSCs from porcine adipose tissue.
- For the first time, we also injected the iPSCs into the myocardium in a porcine model of myocardial infarction and tracked their localization to peri-infarct area by multi-modality MRI and PET/CT imaging.
- In addition, we successfully differentiated porcine iPSCs into endothelial cells (iPSC-ECs) *in vitro* and demonstrated that intra-myocardial injection of iPSC-ECs improved cardiac function in a murine model of myocardial infarction.

Although several groups have created iPSCs from porcine adult tissue, generation of a therapeutic cell type from these large animals has remained challenging. Using a modified protocol for the derivation of human endothelial cells from iPSCs, we successfully generated endothelial cells from porcine iPSCs that shared similar morphological and functional properties as endothelial cells from the aorta. Transplantation of these iPSC-ECs into myocardium in mouse after myocardial infarction resulted in significant improvement in ejection fraction 4 weeks post transplantation. Using a novel microfluidic PCR technique to determine gene expression at the single cell level, we discovered that iPSC-ECs are capable of releasing pro-angiogenic and anti-apoptotic factors in the ischemic environment. These paracrine factors promoted the formation of new blood vessels in the peri-infarct area. We also demonstrated that the pattern of paracrine release varied among different cell subpopulations. In summary, further development of these large animal iPSC models may provide additional insight to facilitate the development of autologous iPSC-based therapy in humans.

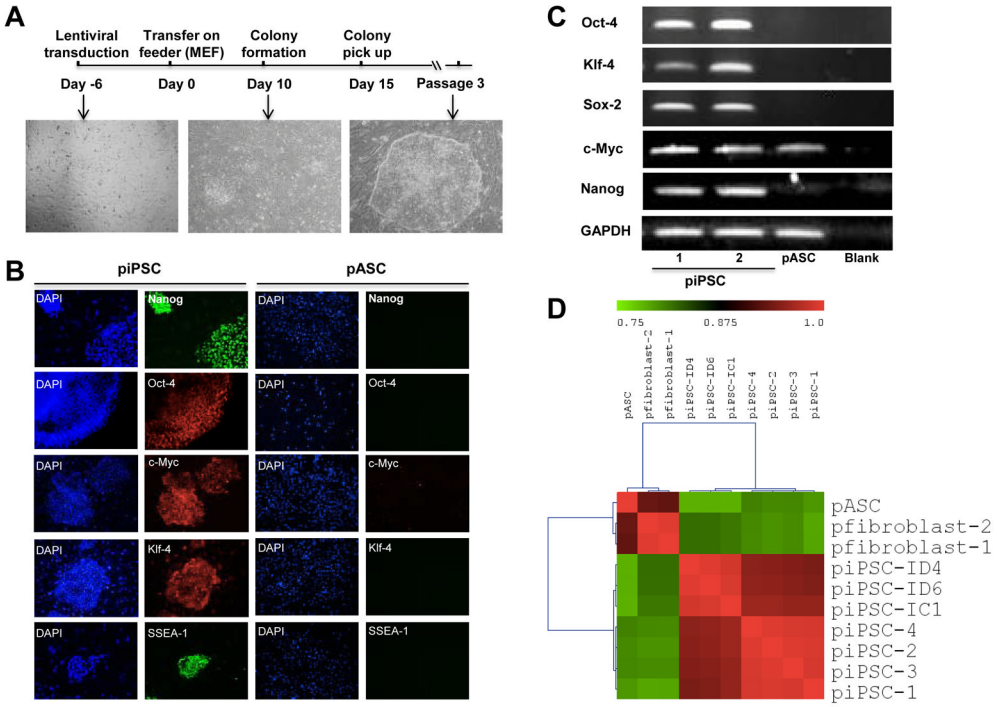

Figure 1. Generation and characterization of porcine induced pluripotent stem cells (piPSCs)

A) Representative timeline of piPSC generation. Compact clones were observed on day 15. **B)** Immunofluorescence staining of pluripotent markers. Unlike the porcine adipose stromal cells (pASCs) from which they were derived, piPSCs stained positive for the traditional markers of pluripotency (e.g., Nanog, Oct4, Klf4 and SSEA-1). pASCs have a weak expression of c-Myc, which is consistent with other reports. **C)** Reverse transcription PCR analysis of pluripotent markers. Expression of Oct4, Klf4, Sox2, and Nanog is present in derived piPSCs, but absent from pASC and negative control (blank). **D)** Pearson correlation analysis for gene expression in piPSCs versus pASCs and porcine fibroblasts (pfibroblasts). Hierarchical clustering of whole genome expression showed that our generated piPSC lines were similar to reference piPSC lines (piPSC-IC1, piPSC-ID4, and piPSC-ID6) generated from another laboratory, and were distinct from pfibroblasts and pASCs. The range of Pearson correlation coefficients are displayed in the color bar (*top*).

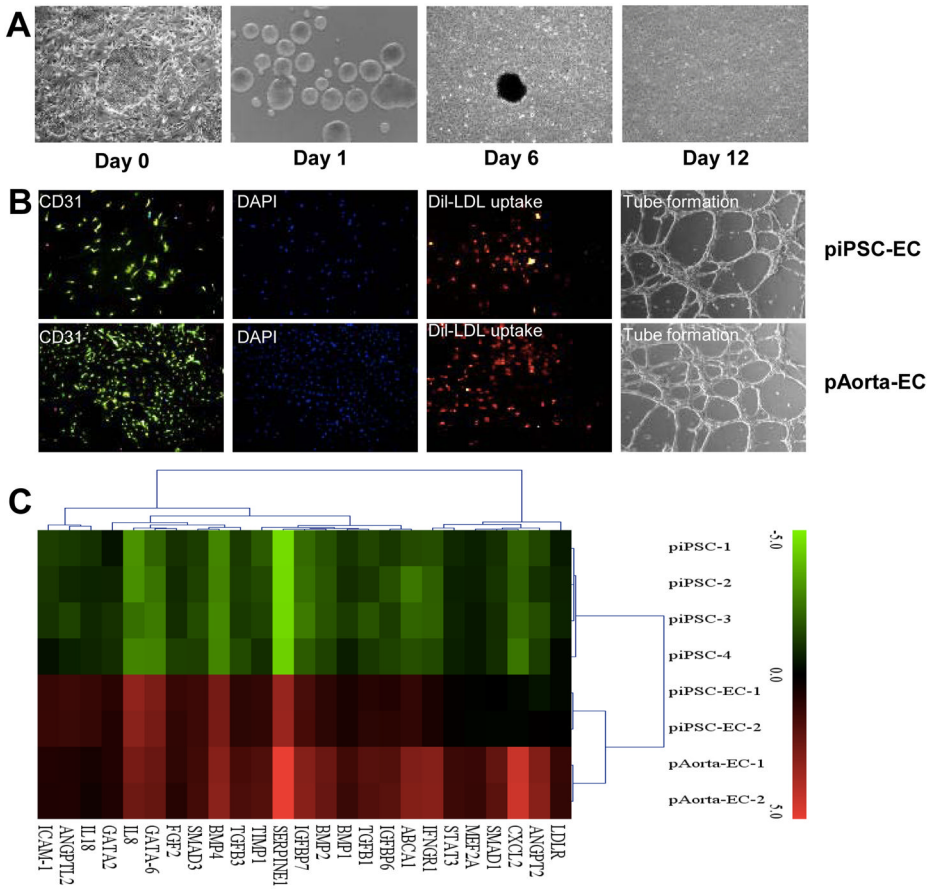

Figure 2. Derivation and characterization of piPSC-derived endothelial cells

A) Bright-field images of endothelial cell differentiation from piPSCs using embryoid bodies. Differentiated cells were dissociated and sorted by FACS on day 12. **B)** Morphological and functional similarities between piPSC-ECs and endothelial cells harvested from the autologous porcine aorta (pAorta-ECs). Both piPSC-ECs and pAorta-ECs show positive immunofluorescence staining for the endothelial marker CD31 (*green*) and DAPI nuclear stain (*blue*). Similar to pAorta-ECs, piPSC-ECs take up acetylated LDL (*red*) and form a capillary-like network on Matrigel 24 hours after seeding the cells (*far right*). **C)** Microarray analysis confirmed that, similar to pAorta-ECs, piPSC-ECs express genes related to endothelial function.

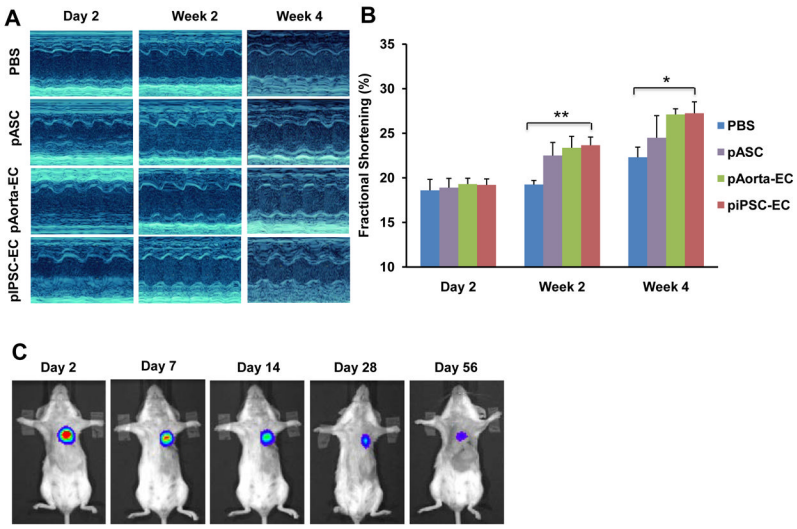

Figure 3. Greater functional improvement noted in mice treated with piPSCs-ECs

A) Representative M-mode echocardiographic views of infarcted hearts receiving PBS, pASCs, pAorta-ECs, and piPSC-ECs (n=20 per group). **B)** Quantification of fractional shortening (FS) reveals significant improvement in systolic function of animals receiving piPSC-ECs at week 2 and week 4 post-MI compared to animals receiving PBS (week 2, 23.7±0.9% vs. 19.3±0.5%, *P<0.01; week 4, 27.2±1.3% vs. 22.3±1.1%, **P<0.001). Greater improvement was also seen in animals receiving piPSCs compared to pASCs although this did not reach statistical significance (week 2, 23.7±0.9% vs. 21.5±1.5%, P=NS; week 4, 27.2±1.3% vs. 24.2±2.5%, P=NS). Comparable improvement is observed between animals receiving piPSC-ECs and their endogenous counterpart, pAorta-ECs (week 2, 23.7±0.9% vs. 23.4±1.3%; week 4, 27.2±1.3% vs. 27.1±0.6%; P=NS). **C)** Representative BLI of an animal receiving 1×10^6 piPSC-ECs demonstrated robust cell engraftment at day 2 following injection. Progressive decrease in signal was observed over the next several weeks, but persistent cell engraftment is still noted at week 4.

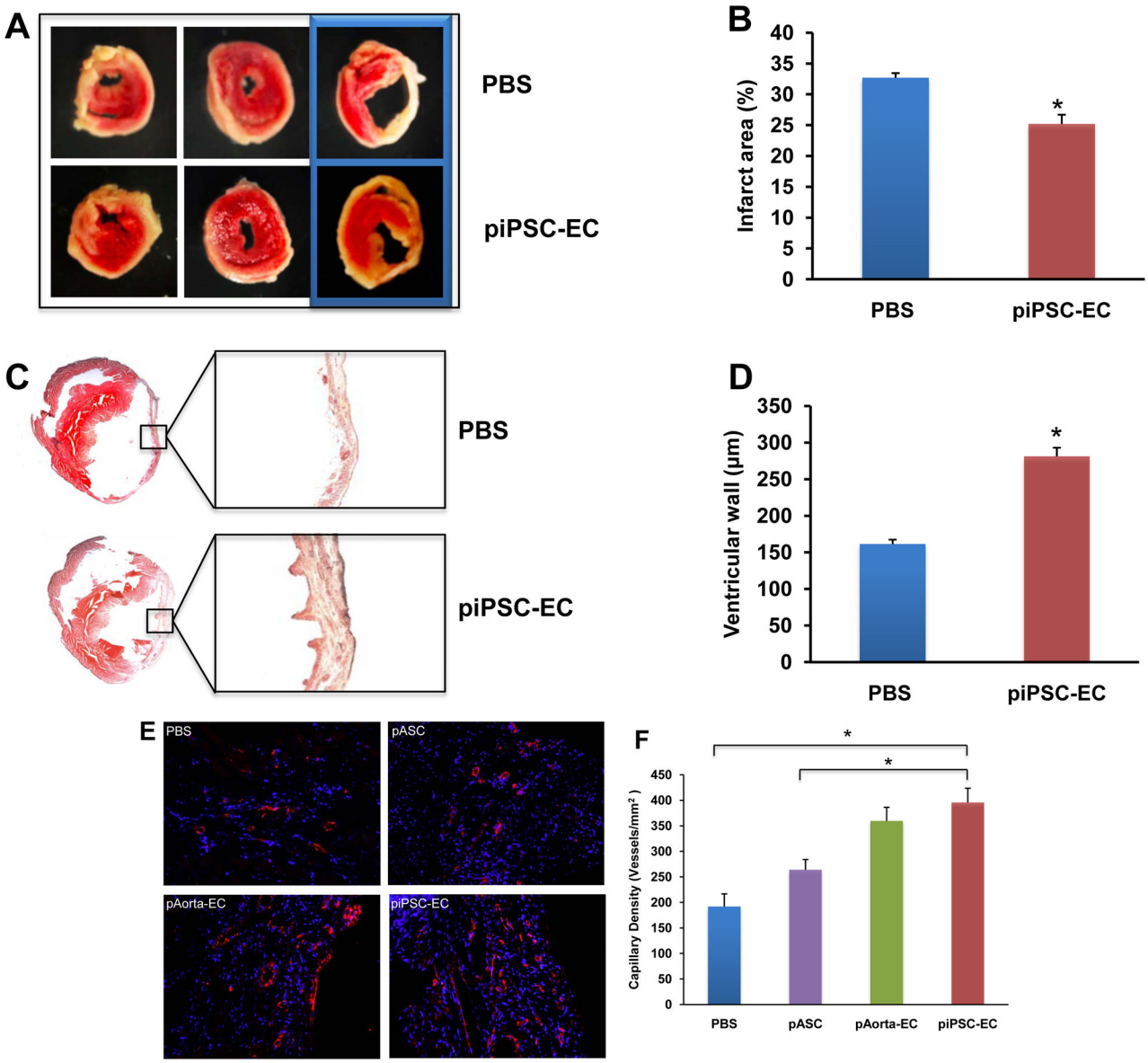

Figure 4. Histological evaluation of piPSC-EC therapy in infarcted hearts at week 4

A) Representative triphenyltetrazolium chloride (TTC) gross histochemical analysis of infarcted hearts injected with PBS (control group) and piPSC-ECs. **B)** Quantitative analysis of the infarct size showed that the percent infarct size is significantly smaller in mice treated with piPSC-EC compared to PBS (25.2±1.5% versus 32.7±0.8%; *P<0.05). **C)** Representative histology of infarcted hearts injected with PBS and piPSC-ECs (hematoxylin and eosin, magnification 1.25x and 5x for the whole heart and left ventricular wall, respectively). **D)** Quantitative analysis of the left ventricular wall thickness showed thicker ventricular walls were present in the piPSC-EC compared to PBS control group (281±12 μm versus 161±6 μm; *P <0.01). **E)** Representative immunofluorescence staining of the murine endothelial marker CD31 in the peri-infarct area of mice treated with PBS, pASCs, pAorta-ECs, and piPSC-ECs. **F)** Quantitative analysis of capillary density (vessel/mm^2) showed a significant increase in vessel density (# vessels per high power field) in animals treated with piPSC-ECs compared to PBS (395±28 vessels/mm^2 versus 107±9 vessels/mm^2,*P<0.001).

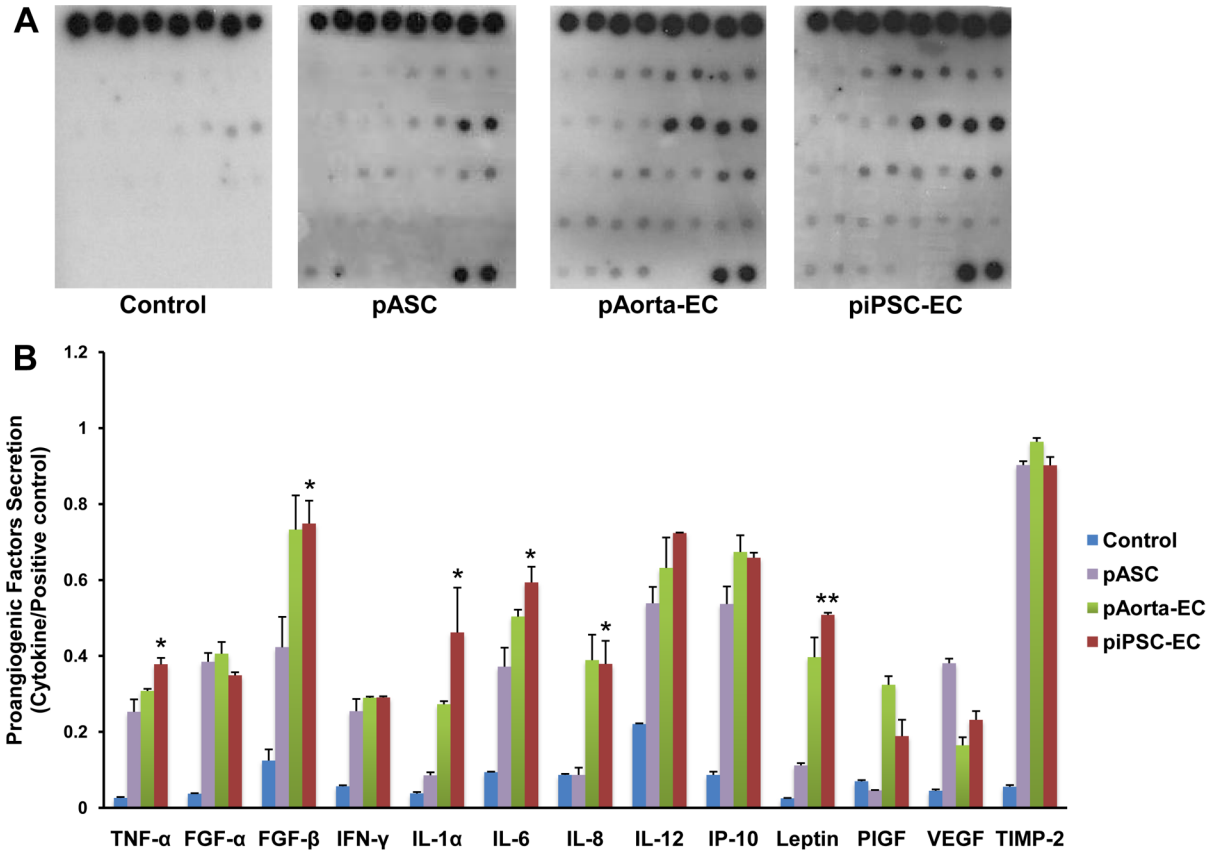

Figure 5. Cytokine expression array demonstrate piPSC-ECs release paracrine factors with *in vitro* hypoxia stress

A) Angiogenesis and anti-apoptosis protein array data after hypoxia exposure for 24 hours. **B)** Quantitative analysis of the cytokine array confirmed significant up-regulation of several pro-angiogenic and anti-apoptotic related proteins in pASCs, pAorta-ECs, and piPSC-ECs compared to control (culture medium without cells under hypoxic conditions). Interestingly, piPSC-ECs released significantly more paracrine factors than pASCs. A similar pattern of paracrine secretion was noted between piPSC-ECs and their endogenous counterparts, pAorta-ECs. Two biological replicates per group (*P<0.05, **P<0.001 vs. pASCs).

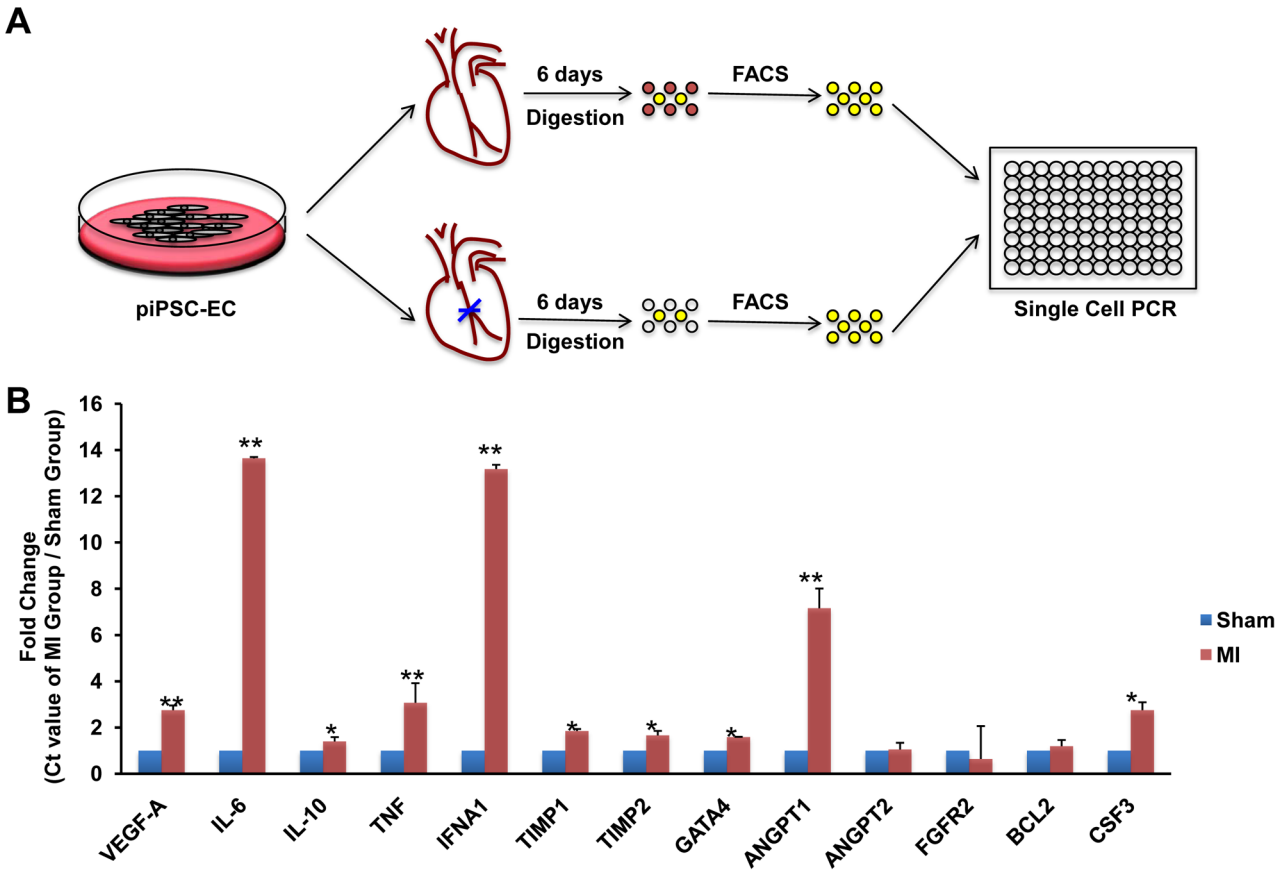

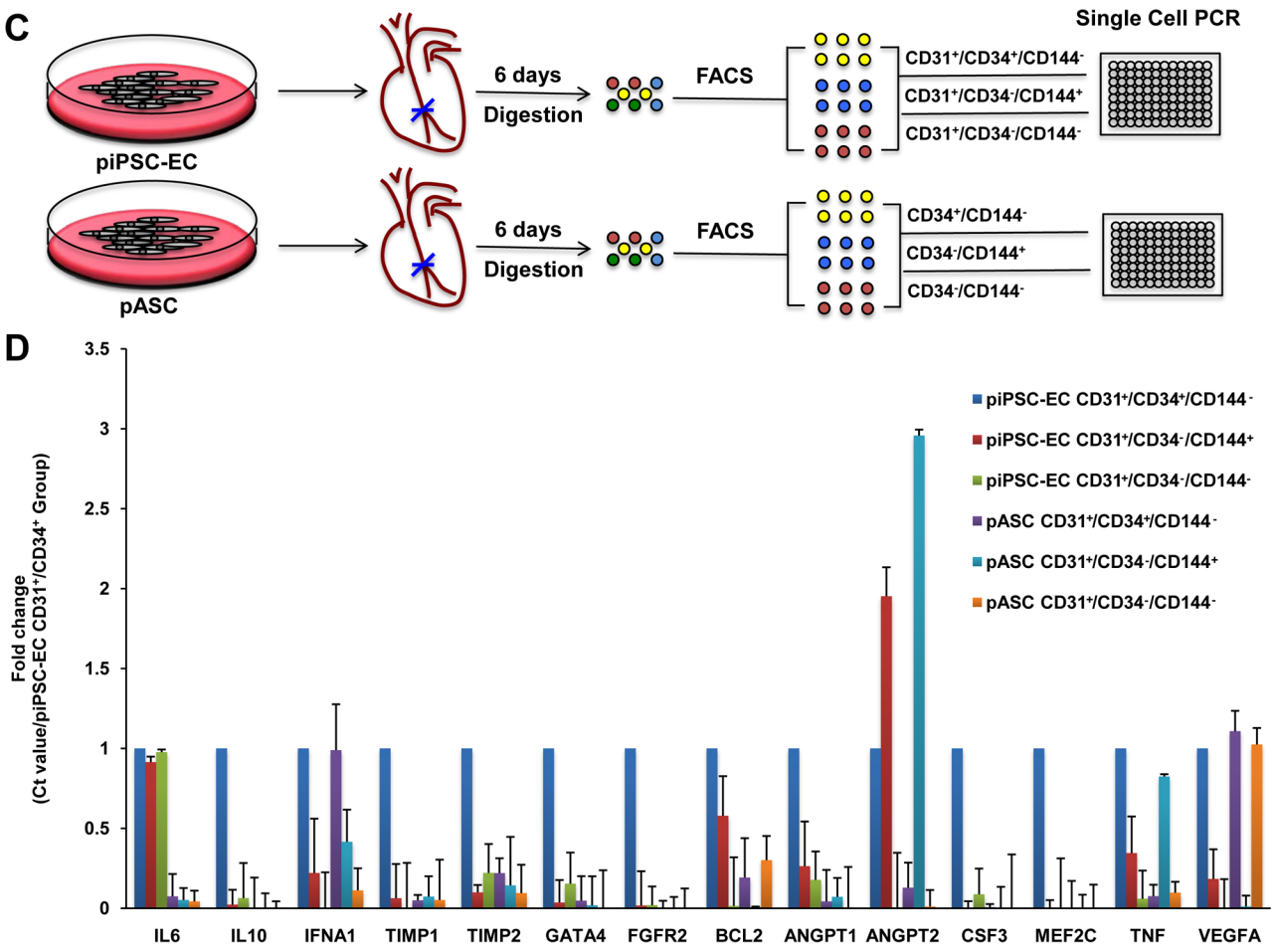

Figure 6. Microfluidic single cell gene expression profiling demonstrates piPSC-ECs can release paracrine factors *in vivo*

A) Schematic outline of single cell expression profiling experiment demonstrating that paracine factors are released in response to the ischemic microenvironment. One-week post injection into normal vs. infarcted hearts, piPSC-ECs were harvested, sorted by FACS, and analyzed by single cell qRT-PCR. **B)** Comparison of fold-change obtained by single cell qRT-PCR showed a significant increase in the expression of 10 genes, which have pro-angiogenic and/ or anti-apoptotic effects, in the MI group compared to the sham group. Fold-change is defined as the Ct value of the MI group divided by the Ct value of the sham group. Results confirm that piPSC-ECs are able to respond to the local ischemic milieu by secreting pro-angiogenic and anti-apoptotic factors. **C)** Schematic outline of single cell expression experiment showing that the release of paracrine factors varied among different subpopulations of pASC and piPSC-ECs. One week post injection into infarcted hearts, injected cells were harvested, subpopulations of pASCs and piPSC-ECs were isolated using FACS and single cell qRT-PCR was performed. **D)** Comparison of fold-change obtained by single cell qRT-PCR showed patterns of paracrine release varied among three populations of piPSC-ECs and ASCs and cells: 1) $CD31^{+}/CD34^{+}/CD144^{-}$, 2) $CD31^{+}/CD34^{-}/CD144^{+}$, and 3) $CD31^{+}/CD34^{-}/CD144^{-}$